JACS
JOURNAL OF THE AMERICAN CHEMICAL SOCIETY

pubs.acs.org/JACS
Communication

Enhancing the Photoswitching Properties of *N*-Alkyl Imines

Jiarong Wu, Lasse Kreimendahl, and Jake L. Greenfield*

Cite This: *J. Am. Chem. Soc.* 2025, 147, 17549−17554
Read Online

ACCESS | Metrics & More | Article Recommendations | Supporting Information

ABSTRACT: *N*-Alkyl imines are prevalent in dynamic-covalent chemistry and self-assembled structures, yet their *E*/*Z* photochromism is often overlooked due to the high-energy light required for isomerization. Here, we present a simple strategy to enhance their photoswitching properties, achieving switching wavelengths and photostationary state distributions comparable to azobenzene. Moreover, we demonstrate that these *N*-alkyl imines undergo photoisomerization in the condensed phase and exhibit isomer-dependent fluorescence. We anticipate that this study will inspire the design of photoresponsive architectures that operate directly at the dynamic-covalent bond, eliminating the need for dedicated photoswitchable motifs.

N-Alkyl imines, specifically *N*-alkyl aldimines, are important motifs in dynamic-covalent (DC) chemistry and have been widely utilized in the assembly of various structures including macrocycles,[1−7] mechanically interlocked molecules,[8] cages[3,9−14] and covalent organic frameworks,[15] and others.[8,16] Recently, there has been growing interest in rendering such imine-containing systems photoresponsive to elicit light-mediated functionality.[1,9,17,18] This has traditionally been achieved by incorporating a dedicated photochromic motif—most commonly azobenzene—that is distinct from the imine linkage.[9,10,19] However, the imine bond (C═N) itself can exhibit photoisomerism,[16,20−23] offering the potential to serve both as the DC linkage and the photoresponsive unit, while also introducing additional light-fueled functionality.[24,25] Despite its promise and simplicity, this approach has been largely overlooked due to two major challenges: (*i*) the *E*/*Z* photoisomerization of imines has historically underperformed compared to other classes of photoswitches in terms of completeness of *E*-to-*Z* switching;[16] (*ii*) *N*-alkyl imines typically require high-energy UV light for photoisomerization,[22,26] complicating their implementation and operation in larger systems and materials—a limitation that arises from their reduced conjugation length relative to *N*-aryl imines, leading to a higher energy $\pi-\pi^*$ transition. Addressing these challenges would offer a new design motif for imine-based photoswitches and provide a novel strategy to generating light-responsive DC structures that function directly at the *N*-alkyl imine.

We recently developed a new generation of imine-based photoswitches with enhanced properties,[20,27] including quantitative *E*-to-*Z* photoisomerization under visible light and thermal half-lives ($t_{1/2}$) of the metastable *Z*-isomer extended from seconds up to 25 h at room temperature (20 °C).[27] These studies focused exclusively on *N*-(hetero)aryl imine derivatives,[28] chosen for their structural similarity to azo-based photoswitches. In contrast, the more widely used *N*-alkyl imines in DC self-assembled structures were initially ruled out as promising candidates due to their anticipated poor performance.[16] Specifically, the lack of conjugation in *N*-alkyl imines, raises the energy of the $\pi-\pi^*$ transition,[26] resulting in a hypsochromic shift in their lowest-energy absorption bands (**1a**, Figure 1c). However, a systematic study into the structure−property relationships in aryliminopyrazoles (AIPs)

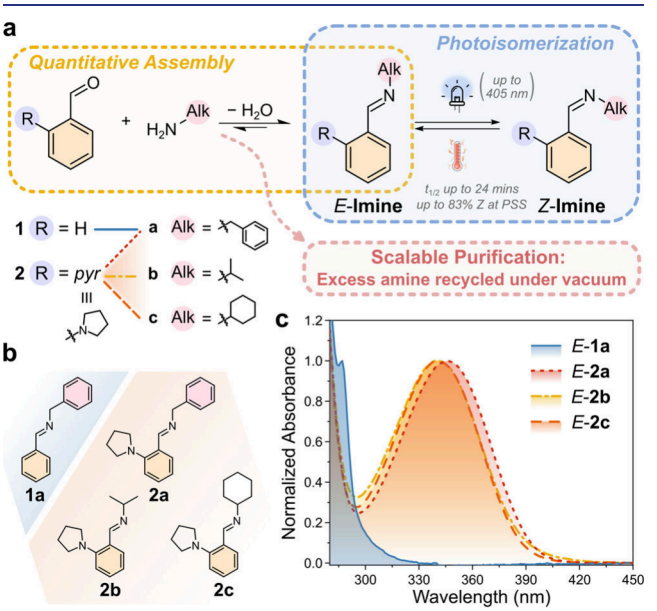

Figure 1. a, Overview of the assembly of the imines via condensation along with their pertinent properties, measured in MeCN. b, Model imines studied in this work. c, Normalized UV/vis absorption spectra (MeCN, 20 °C) of the *E*-imines shown in pane b, highlighting the large bathochromic shift for imines containing the *ortho*-pyrrolidine substituent.

Received: February 9, 2025
Revised: April 26, 2025
Accepted: April 29, 2025
Published: May 15, 2025

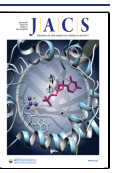

https://doi.org/10.1021/jacs.5c02404
J. Am. Chem. Soc. 2025, 147, 17549−17554

revealed that significant red-shifts in the UV/vis absorption spectrum are largely dictated by the inherent electronic properties of the functionalized phenyl ring.[27] This insight led us to revisit *N*-alkyl imines, hypothesizing that their limitations could be effectively addressed by using a suitable aldehyde component.

In this work, we present a strategy to achieve photochromic *N*-alkyl aldimines with practical photoswitching properties. Specifically, we report photostationary states (PSSs) containing up to 83% of the *Z*-isomer, $t_{1/2}$ values exceeding 20 min at room temperature, and photoswitching enabled by light sources up to 405 nm (in MeCN, photoswitching properties in other solvents are detailed in Section 3.6 of the Supporting Information). Furthermore, we find that these *N*-alkyl derivatives exhibit photoisomerism in the condensed phase and display fluorescence emission in both solution and condensed phases, where the emission correlates with the degree of *E*-to-*Z* photoconversion. We anticipate that these results will renew interest in exploring photoswitchable *N*-alkyl imines, highlighting their potential as promising candidates for integration into light-responsive DC self-assembled structures, unifying the DC and photochromic unit within the same bond.

Building on strategies we developed for creating red-shifted AIP switches,[27] we assembled a series of *N*-alkyl imines featuring *ortho*-pyrrolidine substitution,[20] which exhibit a relatively low-energy $\pi_n-\pi^*$ transition (Figure 1a,b).[29] Imine **1a** was prepared as a reference compound to highlight the significance of this $\pi_n-\pi^*$ transition. Three different amines, **a**−**c**, structurally similar to those commonly used in self-assembled structures, were explored. The imines were synthesized using a one-pot method by combining 1 equiv of the aldehyde component with 1.5 equiv of the *N*-alkyl amine component. While equimolar amounts of amine and aldehyde components are sufficient for imine formation, the use of excess amine accelerated reaction times and ensured quantitative condensation. The resulting mixture was purified by removing the excess amine under vacuum, yielding the desired imines in quantitative yields without requiring further purification. This straightforward and scalable synthesis highlights the accessibility of these *N*-alkyl imine photoswitches. Moreover, the excess amine removed under vacuum was recovered and recycled. The simplicity of this synthesis and purification process makes these *N*-alkyl imines particularly well suited for automated synthesis[30] and high-throughput screening studies.[10,31−33]

The photoswitching properties of these *N*-alkyl imines were first evaluated in solution using MeCN as the solvent. The lowest-energy absorption band for the *N*-alkyl imines **2a**−**2c**, corresponding to a $\pi_n-\pi^*$ transition,[29] was significantly red-shifted, with shifts of up to 59 nm compared to the reference imine **1a** (Figure 1c and Table 1). Generally, the UV/vis absorption spectra of **2a**−**2c** are similar due to the chromophores in these derivatives being comparable and relatively unaffected by the *N*-alkyl component; DFT studies show that the lowest energy electronic transition of the *E*-isomers is localized on the aminated phenyl ring (Figures S28−S31). The bathochromic shift in UV/vis absorption enables **2a**-**2c** to undergo *E*-to-*Z* photoisomerism using wavelengths as long as 405 nm in MeCN (Figure S15, Table S4), substantially longer than those reported for other *N*-alkyl imines (typically ≲310 nm).[22,26] Furthermore, the $\pi_n-\pi^*$ and $n-\pi^*$ absorption bands of the *E*- and *Z*-isomers of **2a**-**2c** are well separated (Figure 2a, Table S2), improving the selective addressability of each isomer with different wavelengths of light.

Table 1. Summary of the Absorbance, Photoswitching, and Fluorescence Properties of the Imines Investigated

		1a	2a	2b	2c
$\lambda_{max,abs}$ (nm)		287	346	340	340
$t_{1/2}$ (min)		-	23.9	8.22	4.34
%*Z* at PSS (385 nm)		-	83%	77%	73%
$\lambda_{max,em}$ (nm)		-	434	428	427
QY *E*-to-*Z* (365 nm)		-	0.50	0.48	0.44
Stokes shift (cm^{-1}) [nm]		-	5860 [88]	6050 [88]	5990 [86]
τ (ns)		-	2.8	1.6	1.3
φ_{PLQY}	solution	-	12.6%	5.8%	5.3%
	solid	-	2.5%	1.1%	1.2%
k_{nr} (s^{-1})		-	3.1×10^8	5.9×10^8	7.3×10^8
k_r (s^{-1})		-	4.5×10^7	3.6×10^7	4.1×10^7

The photoswitching properties could also be tuned by choice of the solvent. The *N*-alkyl imines exhibit positive solvatochromism, showing a 13 nm redshift in the λ_{max} when transitioning from cyclohexane to DMSO (Section 3.6 of the Supporting Information). Notably in DMSO, modest *E*-to-*Z* photoswitching could even be achieved with 430 nm light, resulting in 38% of **2a** as the *Z*-isomer. The $t_{1/2}$ was also found to depend on the solvent, showing trends similar to those observed for AIPs,[20] and supporting an inversion pathway for the thermal *Z*-to-*E* isomerism (Table S7). Again, the use of DMSO stands out, with **2a** exhibiting a $t_{1/2}$ of 2.7 h at 20 °C (Figure S21).

Photochemical action plots, whose utility has been recently revitalized by Barner-Kowollik and co-workers,[34] effectively highlight the wavelength-dependence of photochemical processes. For the *N*-alkyl imines studied here, the action plots reveal a bathochromic shift relative to the UV/vis absorption spectra of the *E*-isomers, and are particularly apparent for **2a** (Figure S19).[35] The quantum yield (QY) of *E*-to-*Z* photoisomerism was relatively high, reaching 0.50 for **2a** (Table 1, Figures S16−S18). In terms of the completeness of *E*-to-*Z* photoswitching, we achieved a maximum %*Z* of 83% at the 385 nm PSS for **2a**. This value is significant—it represents a higher %*Z* achieved using longer-wavelength light compared to previously reported *N*-alkyl imines and, remarkably, surpasses that of azobenzene.[36]

The thermal stability of the metastable *Z*-isomer toward isomerization to the *E*-isomer was significantly enhanced for **2a**−**2c**, as evidenced by the $t_{1/2}$ values of the *Z*-imines at room temperature (20 °C, Table 1).[16] For example, comparing **2c**, which contains an *N*-cyclohexane motif, with its conjugated analogue *N*-phenyl imine[25] reveals a two-orders-of-magnitude longer $t_{1/2}$ for the former. Compound **2a** exhibited the longest $t_{1/2}$, reaching 24 min at room temperature, slightly surpassing the $t_{1/2}$ of the corresponding AIP (*N*-pyrazole)[20] and ca. 500 times longer than that of the corresponding *N*-phenyl imine (possessing *ortho*-pyrrolidine functionalization).[25] These findings demonstrate that a relatively long $t_{1/2}$ can be achieved for these imines without requiring an *N*-pyrazole motif.

The *Z*-to-*E* thermal isomerism proceeds via an inversion pathway,[27,37] characterized by a linear C—N═C(H) motif at the transition state (TS, Figure 2b), which requires the rehybridization of the *N*-atom from sp^2 to sp. The presence of the sp^3 carbon center adjacent to the sp nitrogen atom

https://doi.org/10.1021/jacs.5c02404
J. Am. Chem. Soc. 2025, 147, 17549−17554

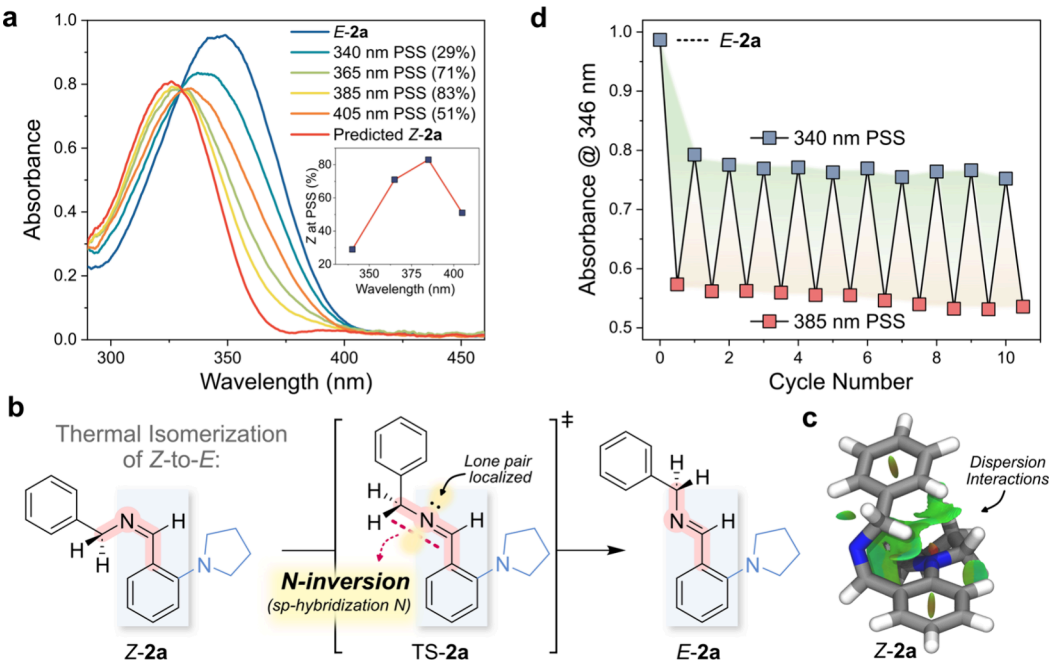

Figure 2. a, UV/vis absorption spectra (260 μM, 20 °C, MeCN) of **2a** at different PSSs. b, Thermal *Z*-to-*E* isomerization of **2a** highlighting the impact of the sp^3 carbon center adjacent to the sp hybridized nitrogen atom in the linear transition state (TS) structure. c, Geometry-optimized structure of *Z*-**2a** with stabilizing noncovalent interaction surfaces shown in green. d, Fatigue resistance of imine **2a** to repeated photoisomerization cycles.

prevents delocalization of the nitrogen's lone pair. In the case of **2a**, the greater flexibility of the *N*-alkyl component enhances dispersive interactions that stabilize the *Z*-isomer. This is evidenced by noncovalent interaction surfaces and the quantification of the E^{D4}_{Z-E} values (Figure 2c, Table S8).[38−40] Consequently, the activation barrier for thermal relaxation is elevated, resulting in a longer $t_{1/2}$ of the *Z*-isomers. The fatigue resistance of imine **2a** is shown in Figure 2c, where the sample was alternately irradiated between the 340 and 385 nm PSSs for 10 cycles (Figure 2d). This combination of enhanced thermal stability of the *Z*-isomer, photostability, and completeness of photoswitching positions these *N*-alkyl imines as promising candidates for light-responsive DC systems without the need for a dedicated photoswitching unit.

Relevant to practical applications,[41] the *N*-alkyl imines also exhibit photoswitching in the condensed phase. Samples were prepared by spin-coating a solution of imine **2a** onto a quartz substrate. The resulting film appeared oily; differential scanning calorimetry (DSC) measurements on **2a** revealed no phase transitions between −70 and 50 °C (Figure S24). These films demonstrated reversible isomerism in the condensed phase (Figure S22); they were cycled five times through *E*-to-*Z* photoisomerism (to the 385 nm PSS) and *Z*-to-*E* thermal relaxation (at 20 °C). A lower %*Z* was achieved in the condensed phase at the 385 nm PSS compared to the solution state (ca. 60% of **2a** as the *Z*-isomer), consistent with the observations of Barner-Kowollik on bis-imines.[26] The ability of these *N*-alkyl imines to isomerize in the condensed phase is particularly promising for their incorporation into materials that are preferred to function without a solvent, for example, the use of porous cages to separate chemicals.[5,6,42,43]

Distinct from AIP and IBP photoswitches,[20,28] solutions of the *N*-alkyl imines exhibit fluorescence behavior and is somewhat similar to the hydrazones of Aprahamian and co-workers (Figure 3a).[44−47] Focusing on **2a**, the excitation spectrum overlaps with the π_n−π^* absorption band of the *E*-isomer, and the excitation and emission bands display a significant Stokes shift of 5860 cm^{-1} (88 nm, Figure 3a). Interestingly, this fluorescence emission is dependent on the isomeric state of the switch, with the *E*-isomer being more emissive than the *Z*-isomer. Consequently, *E*-to-*Z* photoisomerism results in a reversible "photodarkening" process (Figure 3b). This fluorescence property has potential applications in microscopy techniques such as reversible saturable optical fluorescence transitions (RESOLFT),[48] where fluorescence is temporarily suppressed in specific regions to enhance resolution, enabling greater precision in nanoscale imaging.[48]

In solution, the *E*-isomer of imine **2a** exhibits a photoluminescence quantum yield (PLQY) of 12.6% and a fluorescence lifetime of 2.8 ns (Figure S27). Lower PLQYs are observed for **2b** and **2c**, which we infer is due to increased flexibility and vibrational freedom of the *N*-alkyl units, leading to enhanced nonradiative decay (see k_{nr}, Table 1); the radiative rate (k_r) remains similar. Fluorescence emission is retained in the condensed phase, where solution-processed films of **2a** display reversible photodarkening (Table 1, Figure S23). However, the PLQY decreased by approximately 5-fold compared to that in solution. Despite this reduction in the PLQY, the retention of fluorescence and photoswitching ability in the condensed phase underscores their potential for applications in light-responsive materials, where condensed-phase operation is often required. Additionally, the photodarkening behavior provides a readily accessible diagnostic for assessing the degree of photoswitching in real-world applications, without the need for sophisticated instrumentation.

Finally, to demonstrate the accessibility and practical advantages of *N*-alkyl imines—specifically their straightforward synthesis, photoswitching in the condensed phase, and blue-

https://doi.org/10.1021/jacs.5c02404
J. Am. Chem. Soc. 2025, 147, 17549−17554

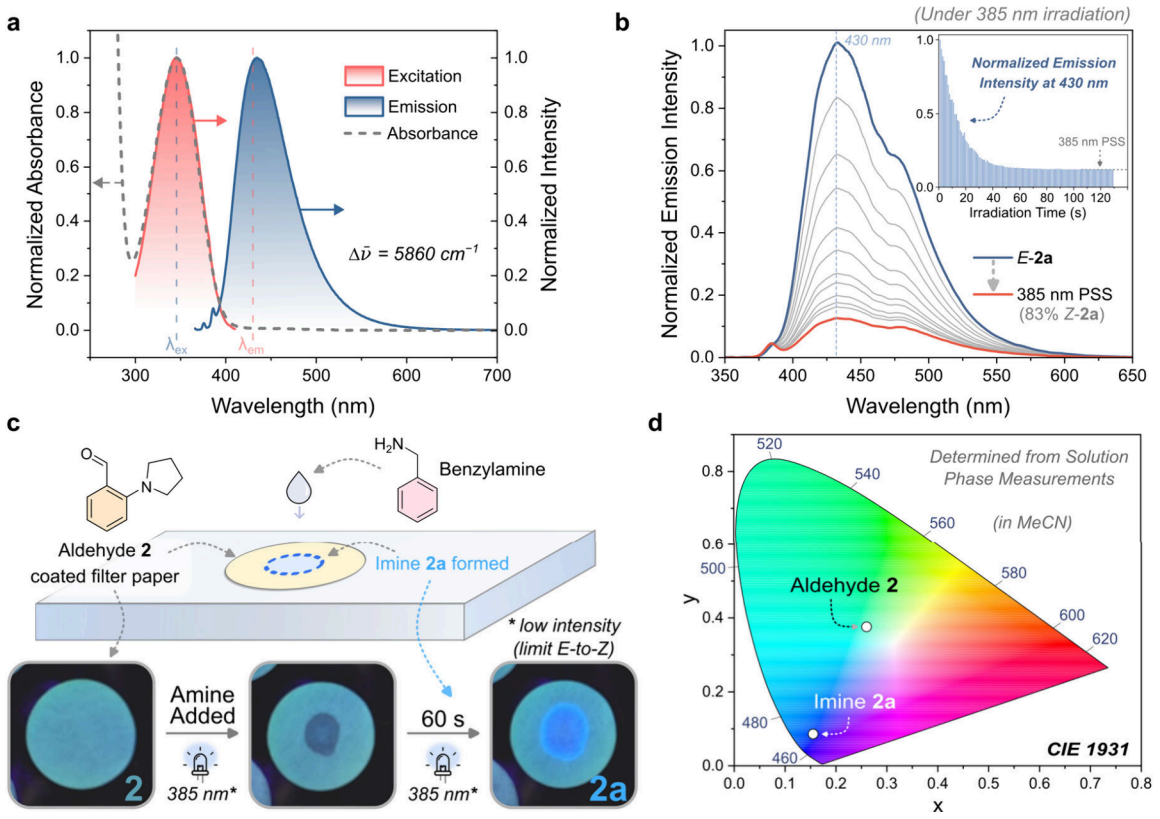

Figure 3. a, Normalized UV/vis absorption spectrum (gray dashed line), normalized fluorescence excitation (red line, λ_{em} = 430 nm) and emission spectrum (blue line, λ_{ex} = 346 nm) of *E*-**2a** (5 μM, 20 °C, MeCN). b, Time-dependent fluorescence emission spectra of **2a** (5 μM, 20 °C, MeCN) under 385 nm photoirradiation. (*inset*) Change in the emission intensity at λ = 430 nm upon *E*-to-*Z* isomerism. c, Schematic of rapid imine formation of **2a**, which was exposed to low-intensity 385 nm light (to limit *E*-to-*Z* photoisomerism) to monitor imine formation. d, The CIE 1931 chromaticity plot showing the difference in perceived emission of aldehyde **2** and imine **2a**.

light fluorescence emission—we prepared a sample of **2a** in real time on a solid substrate (Figure 3c and Video S1). Briefly, a solution of aldehyde **2** in MeCN was deposited onto a piece of filter paper and left to dry. Upon the addition of benzylamine to the aldehyde-coated filter paper via capillary tube, imine condensation occurred within 1 min, resulting in a visible shift in fluorescence emission color from cyan to blue under 385 nm irradiation (Figure 3c and Video S1). This change in color was mapped on the CIE 1931 plot, where the emission of aldehyde **2** is perceived as green/cyan, while imine **2a** is perceived as blue (Figure 3d). Control measurements with substrates containing only the aldehyde, amine, or imine are shown in Video S1. This experiment highlights not only the fluorescent properties of these imines but also their dynamic and reversible nature, allowing for rapid and straightforward synthesis—even directly on a substrate.

In conclusion, we have demonstrated that *N*-alkyl imines, ubiquitous motifs in the field of self-assembly, can exhibit useful photoswitching properties in both solution and condensed phases. Notably, we have shown that they can be prepared effortlessly and at scale, and that this class of imine-based photoswitches exhibits reversible "photodarkening" fluorescence with a large Stokes shift. Putting this work into context, while hydrazone photoswitches—such as those developed by Aprahamian—offer more complete and tunable photoswitching as well as a turn-off fluorescence response in the metastable state,[47] *N*-alkyl imines stand out for their versatility in dynamic-covalent chemistry. Specifically, by combining photoswitching and light-emitting properties with the inherent adaptability of dynamic covalent imine bonds, this work provides a useful toolbox for future applications.[5] Moreover, this could provide an alternative pathway for structural transformations[9,19] that function as an information ratchet[25] rather than an energy ratchet.[9,49,50] Ongoing efforts in our lab are focused on translating these *N*-alkyl imine units into self-assembled architectures, with the goal of achieving higher-order light-responsive changes directly at the imine bond.

■ ASSOCIATED CONTENT

Data Availability Statement

All data that support the findings of this study are included within the article and its Supporting Information and are also available from the authors upon reasonable request.

Supporting Information

The Supporting Information is available free of charge at https://pubs.acs.org/doi/10.1021/jacs.5c02404.

Synthetic details and characterization data (PDF)
Supplementary video (MOV)

■ AUTHOR INFORMATION

Corresponding Author

Jake L. Greenfield − *Institut für Organische Chemie, Universität Würzburg, 97074 Würzburg, Germany; Center for Nanosystems Chemistry (CNC), Universität Würzburg, 97074 Würzburg, Germany;* orcid.org/0000-0002-7650-5414; Email: Jake.Greenfield@uni-wuerzburg.de

https://doi.org/10.1021/jacs.5c02404
J. Am. Chem. Soc. 2025, 147, 17549−17554

Authors

Jiarong Wu − *Institut für Organische Chemie, Universität Würzburg, 97074 Würzburg, Germany; Center for Nanosystems Chemistry (CNC), Universität Würzburg, 97074 Würzburg, Germany;* orcid.org/0000-0002-2701-6526

Lasse Kreimendahl − *Institut für Physikalische und Theoretische Chemie, Universität Würzburg, 97074 Würzburg, Germany;* orcid.org/0009-0009-0020-6897

Complete contact information is available at: https://pubs.acs.org/10.1021/jacs.5c02404

Notes

The authors declare no competing financial interest.

■ ACKNOWLEDGMENTS

This work was funded by the Fonds der Chemischen Industrie (FCI, Liebig Fellowship for J.L.G. and PhD Studentships for J.W. and L.K.). We thank Prof. Frank Würthner for providing infrastructure and Prof. Roland Mitric for computational resources.

■ REFERENCES

(1) Nieland, E.; Voss, J.; Mix, A.; Schmidt, B. M. Photoresponsive Dissipative Macrocycles Using Visible-Light-Switchable Azobenzenes. *Angew. Chem., Int. Ed.* **2022**, *61* (48), No. e202212745.

(2) Ratjen, L.; Vantomme, G.; Lehn, J. Strain-Induced Reactivity in the Dynamic Covalent Chemistry of Macrocyclic Imines. *Chem.—Eur. J.* **2015**, *21* (28), 10070−10081.

(3) Yang, Z.; Esteve, F.; Antheaume, C.; Lehn, J.-M. Dynamic Covalent Self-Assembly and Self-Sorting Processes in the Formation of Imine-Based Macrocycles and Macrobicyclic Cages. *Chem. Sci.* **2023**, *14* (24), 6631−6642.

(4) Scholes, A. M.; Kershaw Cook, L. J.; Szczypiński, F. T.; Luzyanin, K. V.; Egleston, B. D.; Greenaway, R. L.; Slater, A. G. Dynamic and Solid-State Behaviour of Bromoisotrianglimine. *Chem. Sci.* **2024**, *15* (35), 14254−14263.

(5) Zhang, G.; Lin, W.; Huang, F.; Sessler, J.; Khashab, N. M. Industrial Separation Challenges: How Does Supramolecular Chemistry Help? *J. Am. Chem. Soc.* **2023**, *145* (35), 19143−19163.

(6) Dey, A.; Chand, S.; Maity, B.; Bhatt, P. M.; Ghosh, M.; Cavallo, L.; Eddaoudi, M.; Khashab, N. M. Adsorptive Molecular Sieving of Styrene over Ethylbenzene by Trianglimine Crystals. *J. Am. Chem. Soc.* **2021**, *143* (11), 4090−4094.

(7) Dey, A.; Chand, S.; Alimi, L. O.; Ghosh, M.; Cavallo, L.; Khashab, N. M. From Capsule to Helix: Guest-Induced Superstructures of Chiral Macrocycle Crystals. *J. Am. Chem. Soc.* **2020**, *142* (37), 15823−15829.

(8) Jiao, T.; Wu, G.; Zhang, Y.; Shen, L.; Lei, Y.; Wang, C.; Fahrenbach, A. C.; Li, H. Self-Assembly in Water with N-Substituted Imines. *Angew. Chem., Int. Ed.* **2020**, *59* (42), 18350−18367.

(9) Ovalle, M.; Kathan, M.; Toyoda, R.; Stindt, C. N.; Crespi, S.; Feringa, B. L. Light-Fueled Transformations of a Dynamic Cage-Based Molecular System. *Angew. Chem., Int. Ed.* **2023**, *62* (9), No. e202214495.

(10) Brand, M. C.; Trowell, H. G.; Pegg, J. T.; Greenfield, J. L.; Odaybat, M.; Little, M. A.; Haycock, P. R.; Avci, G.; Rankin, N.; Fuchter, M. J.; Jelfs, K. E.; Cooper, A. I.; Greenaway, R. L. Photoresponsive Organic Cages—Computationally Inspired Discovery of Azobenzene-Derived Organic Cages. *J. Am. Chem. Soc.* **2024**, *146* (44), 30332−30339.

(11) Tozawa, T.; Jones, J. T. A.; Swamy, S. I.; Jiang, S.; Adams, D. J.; Shakespeare, S.; Clowes, R.; Bradshaw, D.; Hasell, T.; Chong, S. Y.; Tang, C.; Thompson, S.; Parker, J.; Trewin, A.; Bacsa, J.; Slawin, A. M. Z.; Steiner, A.; Cooper, A. I. Porous Organic Cages. *Nat. Mater.* **2009**, *8* (12), 973−978.

(12) Al Kelabi, D.; Dey, A.; Alimi, L. O.; Piwoński, H.; Habuchi, S.; Khashab, N. M. Photostable Polymorphic Organic Cages for Targeted Live Cell Imaging. *Chem. Sci.* **2022**, *13* (24), 7341−7346.

(13) Alimi, L. O.; Moosa, B.; Lin, W.; Khashab, N. M. Tunable Crystalline Organic Cage for Selective Sorting of Ortho-Monohalotoluene Isomers. *ACS Mater. Lett.* **2024**, *6* (4), 1467−1473.

(14) Sarwa, A.; Białońska, A.; Garbicz, M.; Szyszko, B. Plenates: Anion-Dependent Self-Assembly of the Pyrrole Cage Encapsulating Silver(I) Clusters. *Chem.—Eur. J.* **2023**, *29* (12), e202203850.

(15) Qian, C.; Feng, L.; Teo, W. L.; Liu, J.; Zhou, W.; Wang, D.; Zhao, Y. Imine and Imine-Derived Linkages in Two-Dimensional Covalent Organic Frameworks. *Nat. Rev. Chem.* **2022**, *6* (12), 881−898.

(16) Greb, L.; Vantomme, G.; Lehn, J. Imines as Threefold Functional Devices: Motional, Photochemical, Constitutional. *Molecular Photoswitches*; Wiley: 2022; pp 325−349. DOI: 10.1002/9783527827626.ch15.

(17) Nieland, E.; Voss, J.; Schmidt, B. M. Photoresponsive Supramolecular Cages and Macrocycles. *ChemPlusChem.* **2023**, *88* (12), e202300353.

(18) Kathan, M.; Crespi, S.; Thiel, N. O.; Stares, D. L.; Morsa, D.; de Boer, J.; Pacella, G.; van den Enk, T.; Kobauri, P.; Portale, G.; Schalley, C. A.; Feringa, B. L. A Light-Fuelled Nanoratchet Shifts a Coupled Chemical Equilibrium. *Nat. Nanotechnol.* **2022**, *17* (2), 159−165.

(19) Ovalle, M.; Stindt, C. N.; Feringa, B. L. Light, Switch, Action! The Influence of Geometrical Photoisomerization in an Adaptive Self-Assembled System. *J. Am. Chem. Soc.* **2024**, *146* (46), 31892−31900.

(20) Wu, J.; Kreimendahl, L.; Tao, S.; Anhalt, O.; Greenfield, J. L. Photoswitchable Imines: Aryliminopyrazoles Quantitatively Convert to Long-Lived *Z*-Isomers with Visible Light. *Chem. Sci.* **2024**, *15* (11), 3872−3878.

(21) Han, Z.; He, M.; Wang, G.; Lehn, J.; Li, Q. Visible-Light-Driven Solid-State Fluorescent Photoswitches for High-Level Information Encryption. *Angew. Chem., Int. Ed.* **2024**, *63* (51), e202416363.

(22) Greb, L.; Mutlu, H.; Barner-Kowollik, C.; Lehn, J. M. Photo- and Metallo-Responsive N-Alkyl α-Bisimines as Orthogonally Addressable Main-Chain Functional Groups in Metathesis Polymers. *J. Am. Chem. Soc.* **2016**, *138* (4), 1142−1145.

(23) Georgiev, A.; Yordanov, D.; Dimov, D.; Zhivkov, I.; Nazarova, D.; Weiter, M. Azomethine Phthalimides Fluorescent E→Z Photoswitches. *J. Photochem. Photobiol. A Chem.* **2020**, *393*, 112443.

(24) Greb, L.; Lehn, J.-M. Light-Driven Molecular Motors: Imines as Four-Step or Two-Step Unidirectional Rotors. *J. Am. Chem. Soc.* **2014**, *136* (38), 13114−13117.

(25) Wu, J.; Greenfield, J. L. Photoswitchable Imines Drive Dynamic Covalent Systems to Nonequilibrium Steady States. *J. Am. Chem. Soc.* **2024**, *146* (30), 20720−20727.

(26) Thai, L. D.; Guimaraes, T. R.; Chambers, L. C.; Kammerer, J. A.; Golberg, D.; Mutlu, H.; Barner-Kowollik, C. Molecular Photoswitching of Main-Chain α-Bisimines in Solid-State Polymers. *J. Am. Chem. Soc.* **2023**, *145* (27), 14748−14755.

(27) Wu, J.; Kreimendahl, L.; Greenfield, J. L. Switching Sides: Regiochemistry and Functionalization Dictate the Photoswitching Properties of Imines. *Angew. Chem., Int. Ed.* **2025**, *64* (3), No. e202415464.

(28) Wu, J.; Li, C.; Kreimendahl, L.; Greenfield, J. L. Iminobispyrazole (IBP) Photoswitches: Two Pyrazole Rings Can Be Better than One. *Chem. Commun.* **2024**, *60* (85), 12365−12368.

(29) Zhang, Z.-Y.; Dong, D.; Bösking, T.; Dang, T.; Liu, C.; Sun, W.; Xie, M.; Hecht, S.; Li, T. Solar Azo-Switches for Effective E → Z Photoisomerization by Sunlight. *Angew. Chem., Int. Ed.* **2024**, *63* (31), No. e202404528.

(30) Dai, T.; Vijayakrishnan, S.; Szczypiński, F. T.; Ayme, J.-F.; Simaei, E.; Fellowes, T.; Clowes, R.; Kotopanov, L.; Shields, C. E.; Zhou, Z.; Ward, J. W.; Cooper, A. I. Autonomous Mobile Robots for Exploratory Synthetic Chemistry. *Nature* **2024**, *635* (8040), 890−897.

(31) Greenaway, R. L.; Santolini, V.; Bennison, M. J.; Alston, B. M.; Pugh, C. J.; Little, M. A.; Miklitz, M.; Eden-Rump, E. G. B.; Clowes, R.; Shakil, A.; Cuthbertson, H. J.; Armstrong, H.; Briggs, M. E.; Jelfs, K. E.; Cooper, A. I. High-Throughput Discovery of Organic Cages and Catenanes Using Computational Screening Fused with Robotic Synthesis. *Nat. Commun.* **2018**, *9* (1), 2849.
(32) Abet, V.; Szczypiński, F. T.; Little, M. A.; Santolini, V.; Jones, C. D.; Evans, R.; Wilson, C.; Wu, X.; Thorne, M. F.; Bennison, M. J.; Cui, P.; Cooper, A. I.; Jelfs, K. E.; Slater, A. G. Inducing Social Self-Sorting in Organic Cages To Tune The Shape of The Internal Cavity. *Angew. Chem., Int. Ed.* **2020**, *59* (38), 16755−16763.
(33) Basford, A. R.; Bennett, S. K.; Xiao, M.; Turcani, L.; Allen, J.; Jelfs, K. E.; Greenaway, R. L. Streamlining the Automated Discovery of Porous Organic Cages. *Chem. Sci.* **2024**, *15* (17), 6331−6348.
(34) Irshadeen, I. M.; Walden, S. L.; Wegener, M.; Truong, V. X.; Frisch, H.; Blinco, J. P.; Barner-Kowollik, C. Action Plots in Action: In-Depth Insights into Photochemical Reactivity. *J. Am. Chem. Soc.* **2021**, *143* (50), 21113−21126.
(35) Walden, S. L.; Carroll, J. A.; Unterreiner, A.; Barner-Kowollik, C. Photochemical Action Plots Reveal the Fundamental Mismatch Between Absorptivity and Photochemical Reactivity. *Adv. Sci.* **2024**, *11* (3), 2306014.
(36) Beharry, A. A.; Woolley, G. A. Azobenzene Photoswitches for Biomolecules. *Chem. Soc. Rev.* **2011**, *40* (8), 4422.
(37) Luo, Y.; Utecht, M.; Dokić, J.; Korchak, S.; Vieth, H.-M. M.; Haag, R.; Saalfrank, P. Cis-Trans Isomerisation of Substituted Aromatic Imines: A Comparative Experimental and Theoretical Study. *ChemPhysChem* **2011**, *12* (12), 2311−2321.
(38) Boto, R. A.; Peccati, F.; Laplaza, R.; Quan, C.; Carbone, A.; Piquemal, J.-P.; Maday, Y.; Contreras-Garcıa, J. NCIPLOT4: Fast, Robust, and Quantitative Analysis of Noncovalent Interactions. *J. Chem. Theory Comput.* **2020**, *16* (7), 4150−4158.
(39) Calbo, J.; Weston, C. E.; White, A. J. P. P.; Rzepa, H. S.; Contreras-García, J.; Fuchter, M. J. Tuning Azoheteroarene Photoswitch Performance through Heteroaryl Design. *J. Am. Chem. Soc.* **2017**, *139* (3), 1261−1274.
(40) Caldeweyher, E.; Mewes, J.-M.; Ehlert, S.; Grimme, S. Extension and Evaluation of the D4 London-Dispersion Model for Periodic Systems. *Phys. Chem. Chem. Phys.* **2020**, *22* (16), 8499−8512.
(41) Gonzalez, A.; Kengmana, E. S.; Fonseca, M. V.; Han, G. G. D. Solid-State Photoswitching Molecules: Structural Design for Isomerization in Condensed Phase. *Mater. Today Adv.* **2020**, *6*, 100058.
(42) Moosa, B.; Alimi, L. O.; Shkurenko, A.; Fakim, A.; Bhatt, P. M.; Zhang, G.; Eddaoudi, M.; Khashab, N. M. A Polymorphic Azobenzene Cage for Energy-Efficient and Highly Selective *p*-Xylene Separation. *Angew. Chem., Int. Ed.* **2020**, *59* (48), 21367−21371.
(43) Zhang, G.; Hua, B.; Dey, A.; Ghosh, M.; Moosa, B. A.; Khashab, N. M. Intrinsically Porous Molecular Materials (IPMs) for Natural Gas and Benzene Derivatives Separations. *Acc. Chem. Res.* **2021**, *54* (1), 155−168.
(44) Tatum, L. A.; Su, X.; Aprahamian, I. Simple Hydrazone Building Blocks for Complicated Functional Materials. *Acc. Chem. Res.* **2014**, *47* (7), 2141−2149.
(45) Qian, H.; Pramanik, S.; Aprahamian, I. Photochromic Hydrazone Switches with Extremely Long Thermal Half-Lives. *J. Am. Chem. Soc.* **2017**, *139* (27), 9140−9143.
(46) Shao, B.; Aprahamian, I. Hydrazones as New Molecular Tools. *Chem.* **2020**, *6* (9), 2162−2173.
(47) Shao, B.; Baroncini, M.; Qian, H.; Bussotti, L.; Di Donato, M.; Credi, A.; Aprahamian, I. Solution and Solid-State Emission Toggling of a Photochromic Hydrazone. *J. Am. Chem. Soc.* **2018**, *140* (39), 12323−12327.
(48) Bodén, A.; Ollech, D.; York, A. G.; Millett-Sikking, A.; Testa, I. Super-Sectioning with Multi-Sheet Reversible Saturable Optical Fluorescence Transitions (RESOLFT) Microscopy. *Nat. Methods* **2024**, *21* (5), 882−888.
(49) Borsley, S.; Leigh, D. A.; Roberts, B. M. W. Molecular Ratchets and Kinetic Asymmetry: Giving Chemistry Direction. *Angew. Chem., Int. Ed.* **2024**, *63* (23), No. e202400495.
(50) Sangchai, T.; Al Shehimy, S.; Penocchio, E.; Ragazzon, G. Artificial Molecular Ratchets: Tools Enabling Endergonic Processes. *Angew. Chem., Int. Ed.* **2023**, *62* (47), No. e202309501.

https://doi.org/10.1021/jacs.5c02404
J. Am. Chem. Soc. 2025, 147, 17549−17554